Supporting Information

Ultra-thin carbon-shell coated Ru/RuO_2@C with rich grain boundaries for efficient and durable acidic water oxidation

Qian Chen, Ruonan Wang, Lin Liu, Zhiming Guan, Zhibin Zhu*[a], Lixin Cao*[a], Bohua Dong*[a]

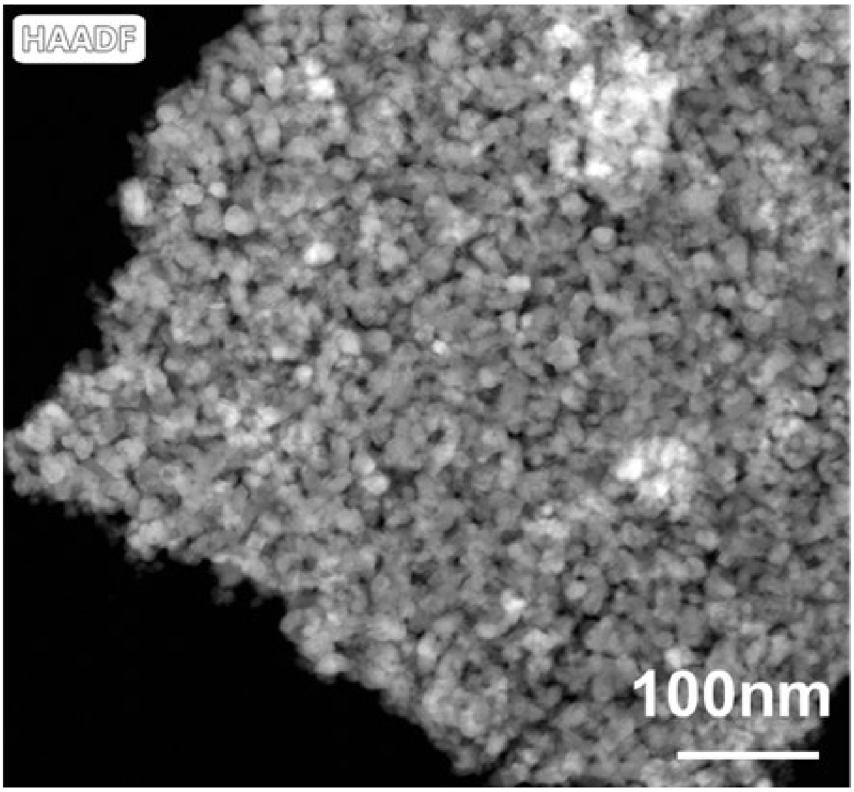

Figure S1. HAADF-STEM image of Ru/RuO_2@C-300.

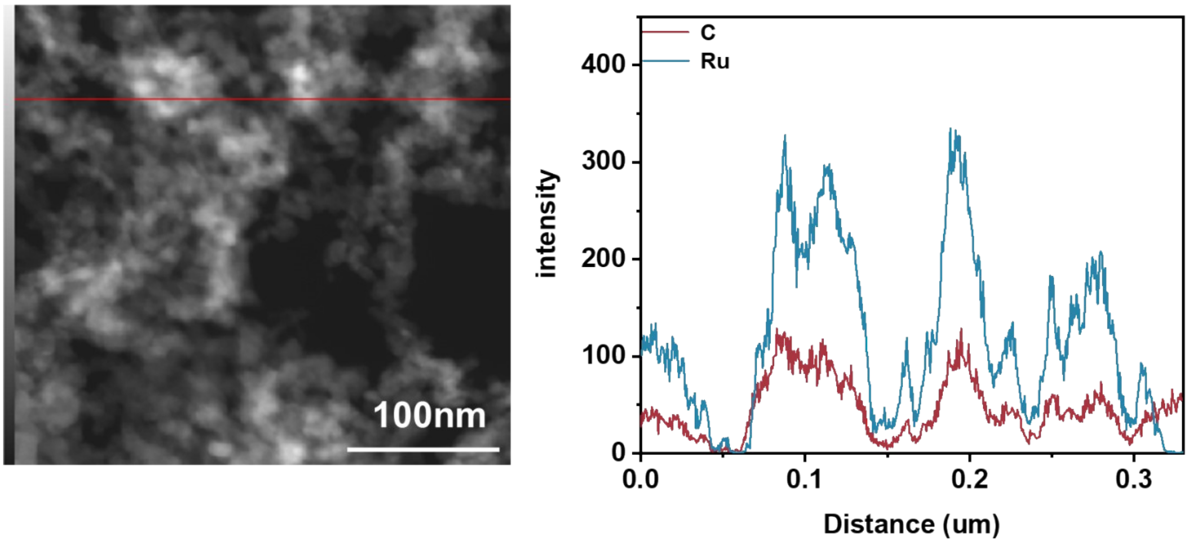

Figure S2. EDS line scan of Ru/RuO_2@C-300.

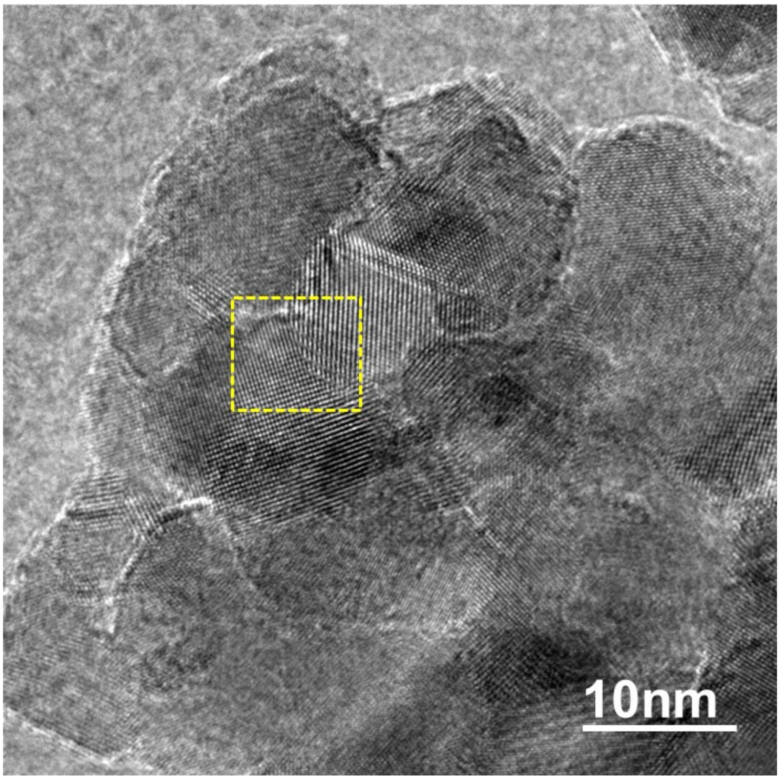

Figure S3. The HRTEM images of Ru/RuO_2@C-300.

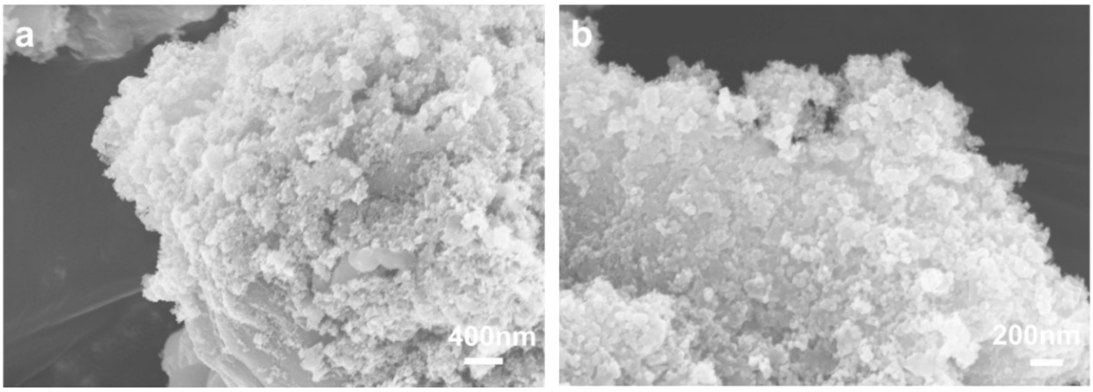

Figure S4. (a)-(b) SEM image of Ru@C.

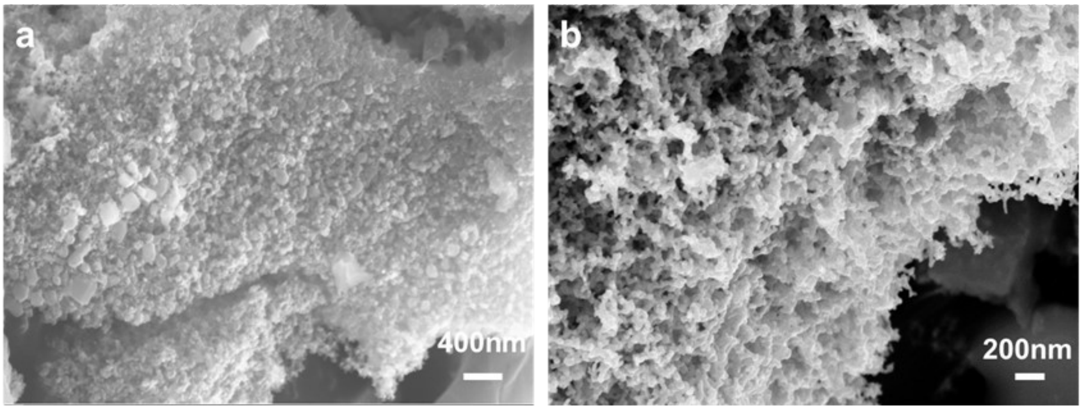

Figure S5. (a)-(b) SEM image of Ru/RuO_2@C-250.

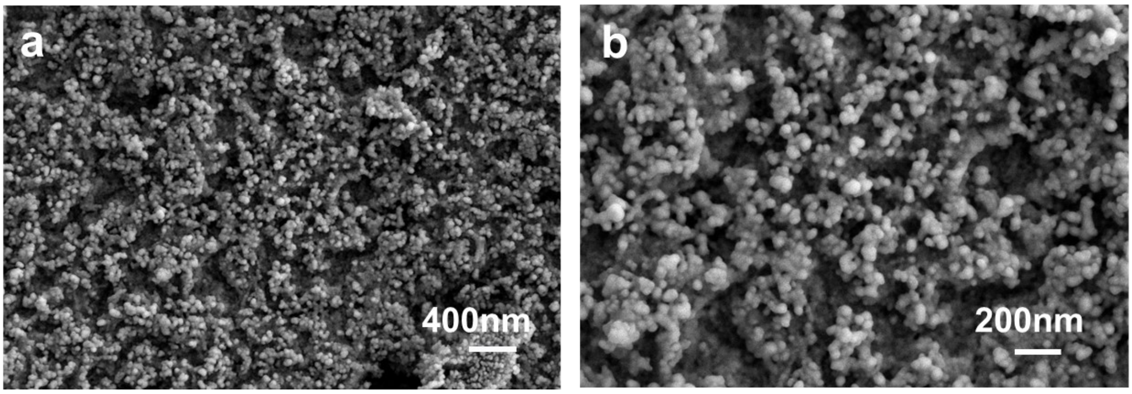

Figure S6. (a)-(b) SEM image of Ru/RuO$_2$@C-300.

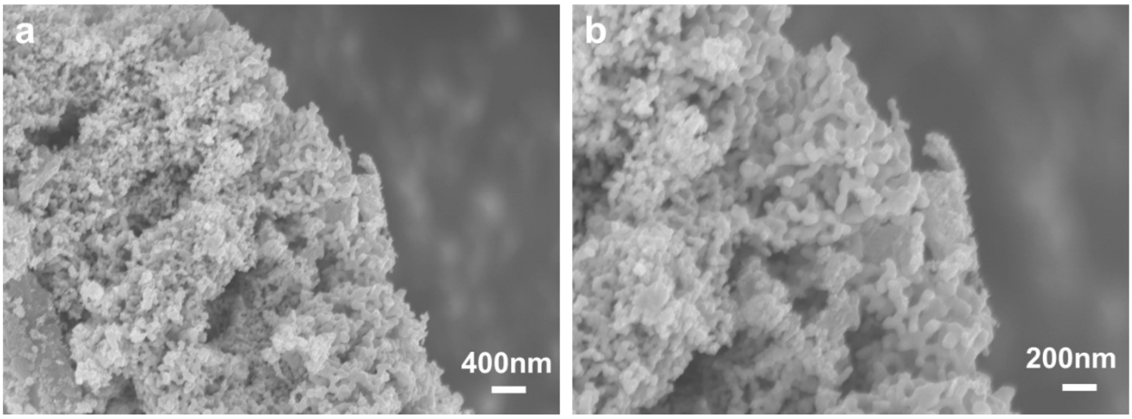

Figure S7. (a)-(b) SEM image of Ru/RuO$_2$@C-350.

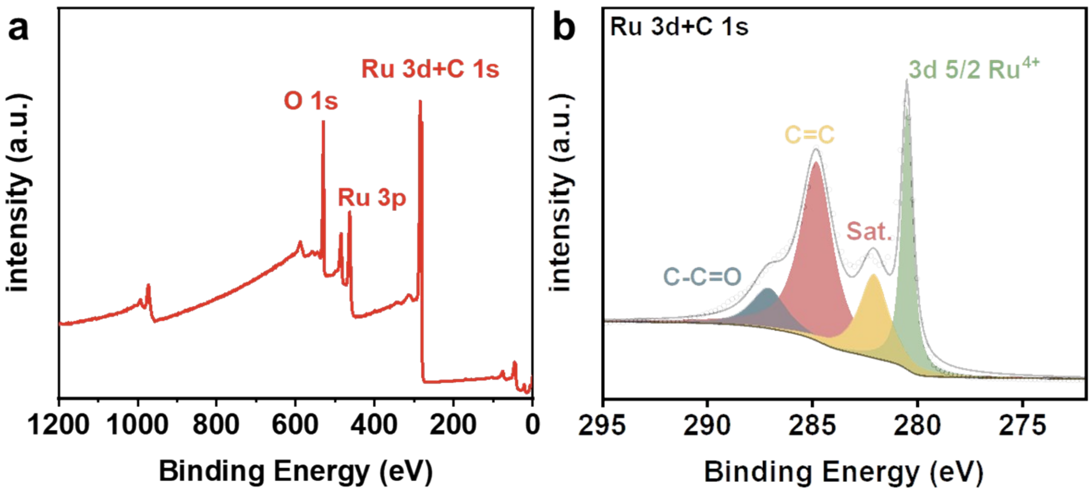

Figure S8. (a) XPS survey, (b) Ru 3d+C 1s of Ru/RuO_2@C-300.

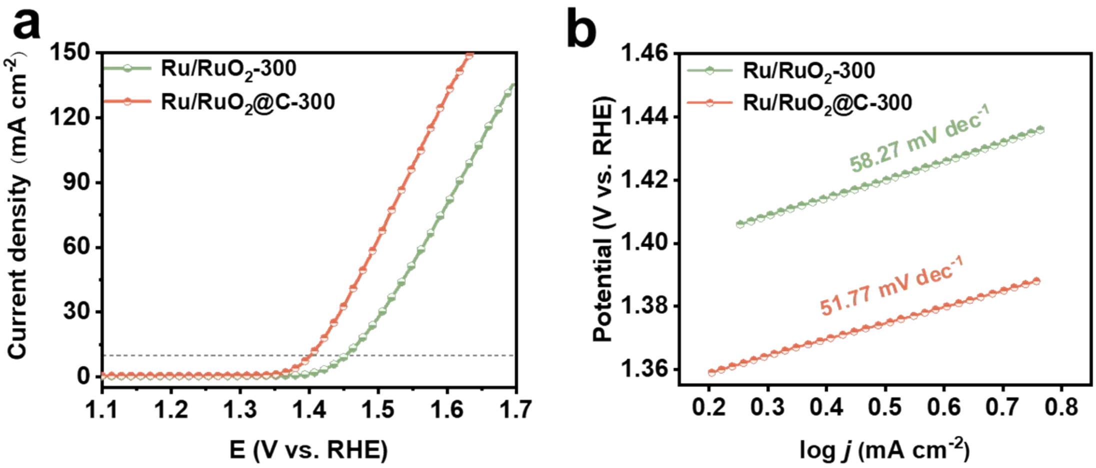

Figure S9. Electrocatalytic performance of Ru/RuO$_2$@C-300 and Ru/RuO$_2$-300 catalysts in 0.5 M H_2SO_4 solution with 90% iR compensation (a) LSV polarization curves. (b) Tafel plots.

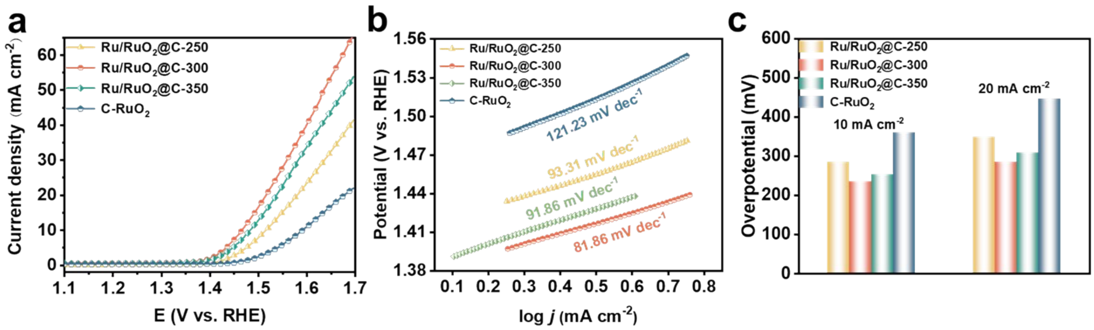

Figure S10. Electrocatalytic performance of Ru/RuO$_2$@C-250, Ru/RuO$_2$@C-300, Ru/RuO$_2$@C-350, and commercial RuO$_2$ catalysts in 0.5 M H_2SO_4 solution without iR compensation (a) LSV polarization curves. (b) Tafel plots. (c) Overpotentials at a current density of 10 mA cm^{-2} and 20 mA cm^{-2}.

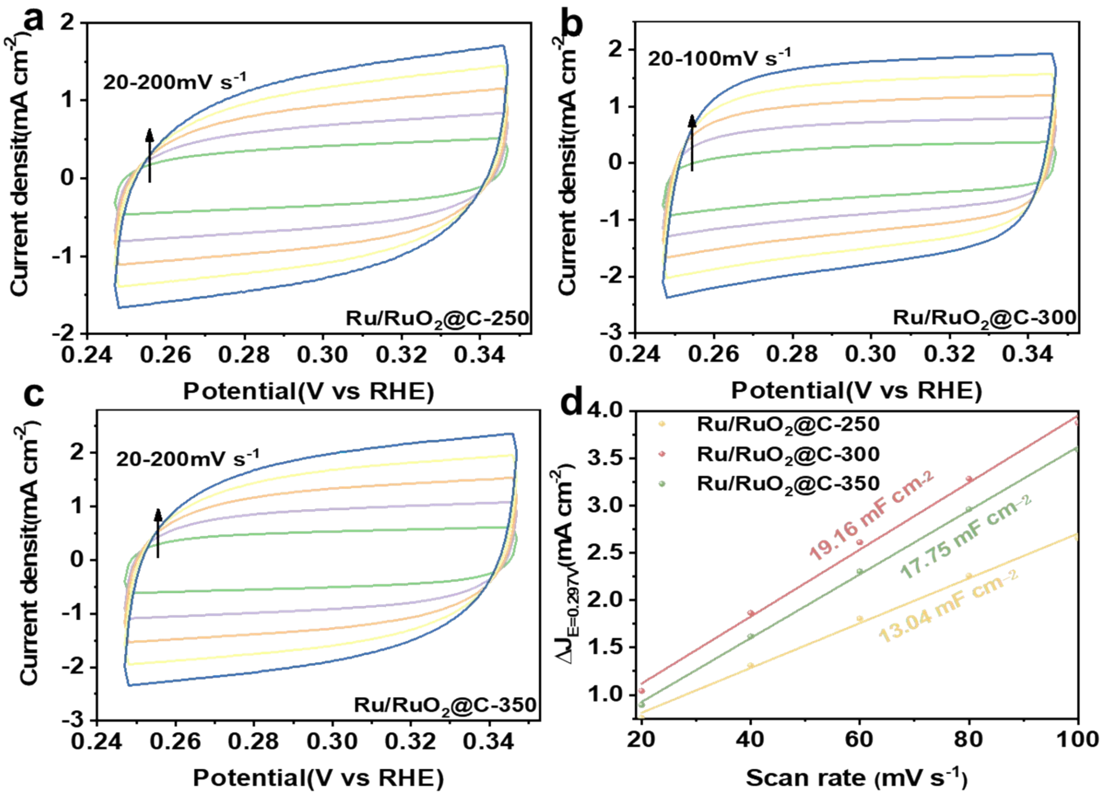

Figure S11. The CV curves of Ru/RuO_2@C-250 (a), Ru/RuO_2@C-300 (b), and Ru/RuO_2@C-350 (c) with the scan rate ranging from 20 to 100 mV s^{-1} in 0.5 M H_2SO_4, the Cdl values at the potential of 0.297 V (d).

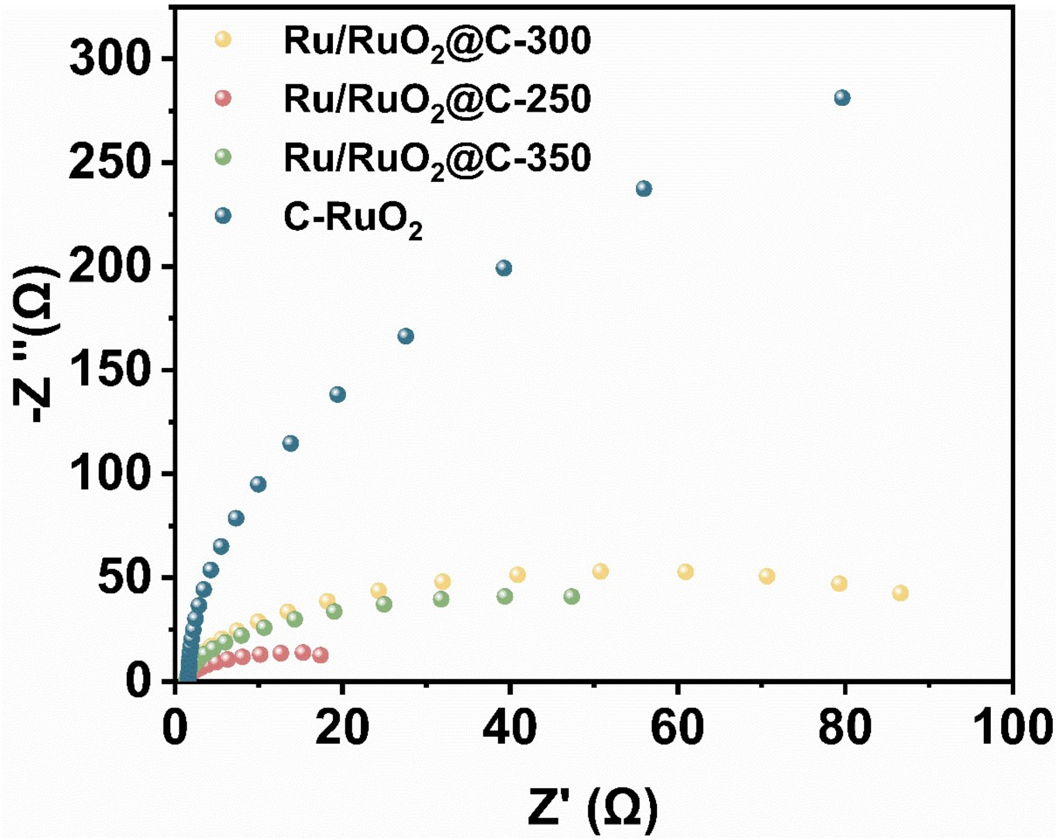

Figure S12. EIS plots of Ru/RuO_2@C-250, Ru/RuO_2@C-300, Ru/RuO_2@C-350 and C-RuO_2.

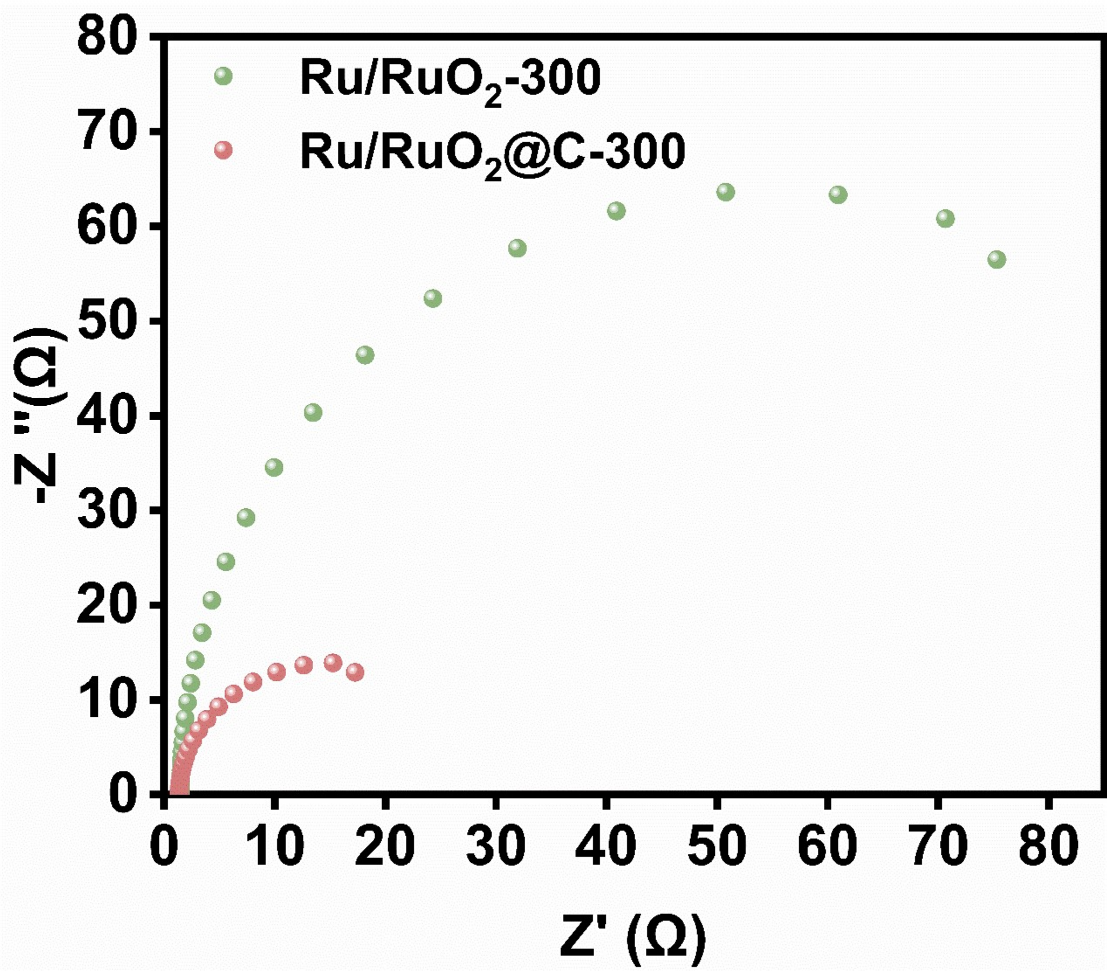

Figure S13. EIS plots of Ru/RuO_2@C-300 and Ru/RuO_2-300.

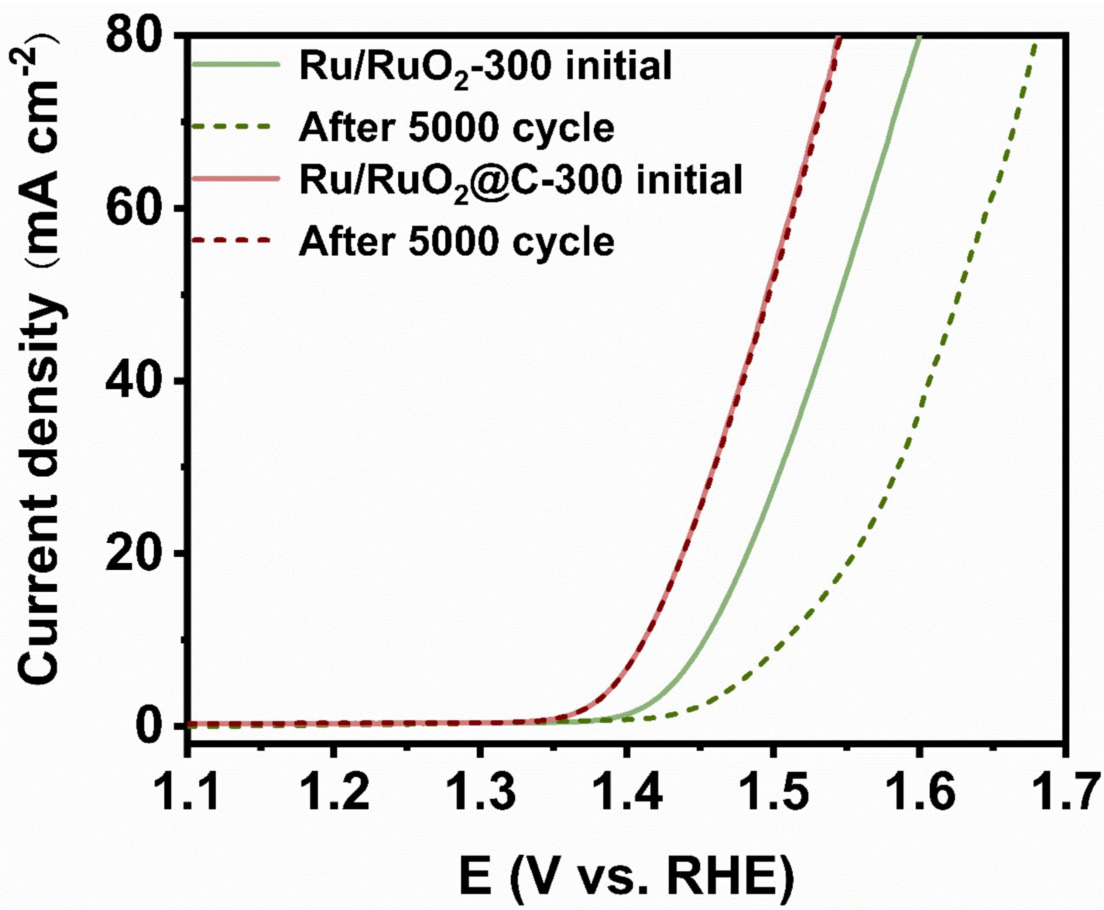

Figure S14. Linear sweep voltammograms of the Ru/RuO_2@C-300 and Ru/RuO_2-300 for OER were obtained before and after 5000 potential cycles.

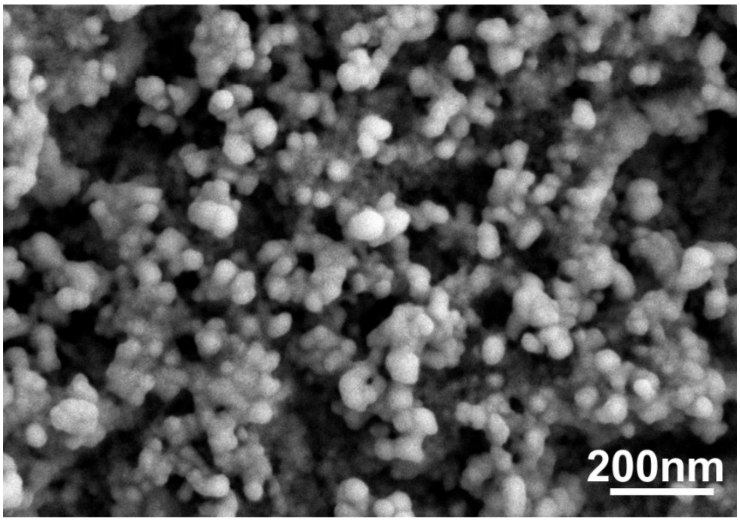

Figure S15. SEM images of the Ru/RuO_2@C-300 after the chronopotentiometry experiment.

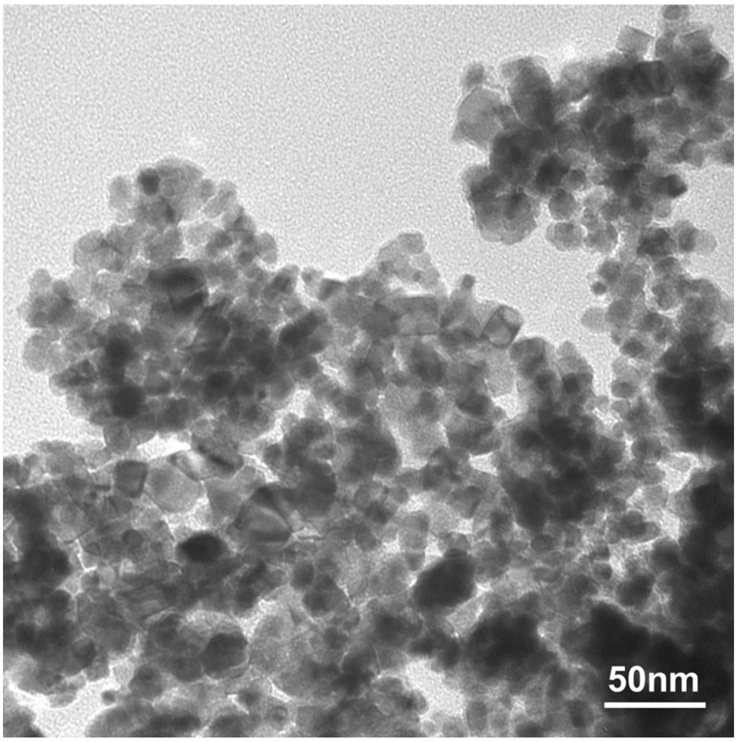

Figure S16. TEM images of the Ru/RuO_2@C-300 after the chronopotentiometry experiment.

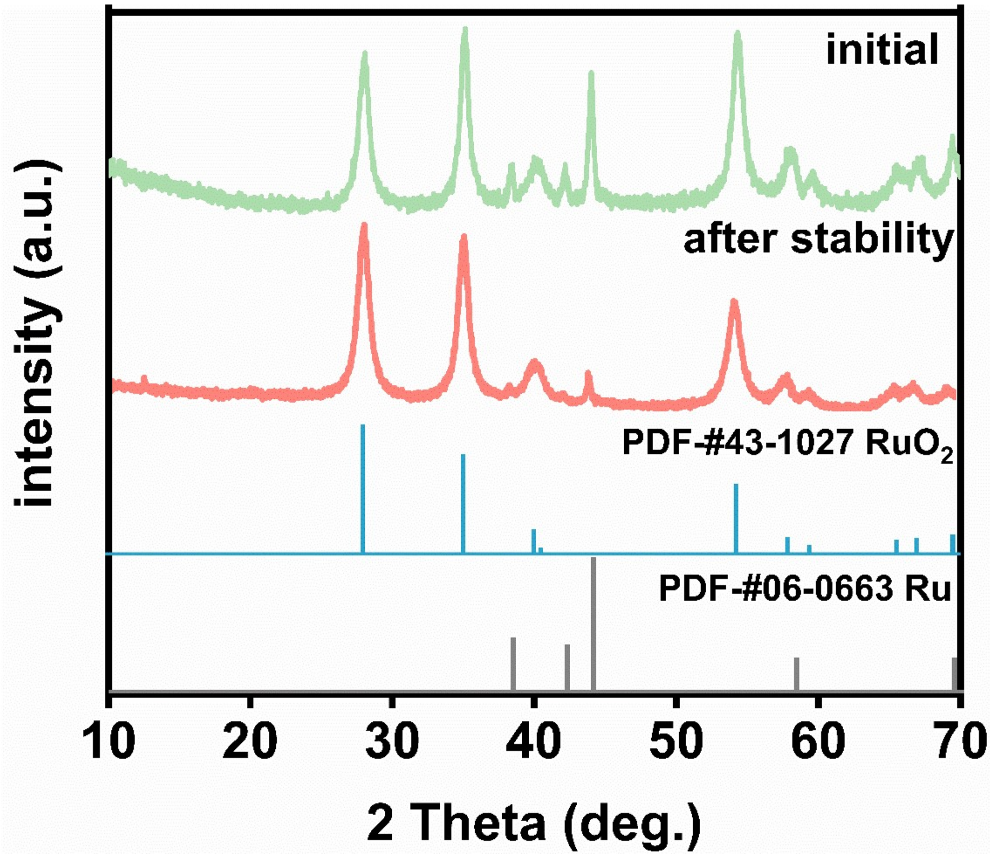

Figure S17. XRD for initial Ru/RuO_2@C-300 and after stability Ru/RuO_2@C-300.

Table S1. Performance comparison of Ru/RuO_2@C-300 with the state-of-art catalysts reported recently in acidic electrolytes.

Catalyst	Electrolyte	η_{10} (mV)	Tafel plots (mV dec^{-1})	Stability (h)	Ref.
Ru/RuO_2@C-300	0.5M H_2SO_4	173	51.77	120@10mA cm^{-2}	This Work
$Cu_{0.3}Ir_{0.7}O_{\delta}$	0.1 M $HClO_4$	351	63	1.67h@ 1.68 V v.s. RHE	1
IrO_2@RuO_2	0.5M H_2SO_4	270	57.8	1000 cycles@ 0.3-1.2 V v.s. RHE	2
1D-RuO_2-CNx	0.5M H_2SO_4	250	52	50 h@ 1.57 V v.s. RHE	3
$Ir_1Fe_{0.11}$/C	0.5 M $HClO_4$	278	62	3.6h @ 10 mA cm^{-2}	4
Ir-$Ni_{0.57}Fe_{0.82}$	0.5 M $HClO_4$	284	48.6	5.6 h @ 10 mA cm^{-2}	5
Ir nanoparticles	0.5M H_2SO_4	290	46	10 h @ 10 mA cm^{-2}	6
RuO_2/Co_3O_4–RuCo@NC	0.5M H_2SO_4	247	89	8 h @ 10 mA cm^{-2}	7
0..27-RuO2@C	0.5M H_2SO_4	220	66		8
$Y_{1.85}Ba_{0.15}Ru_2O_7$	0.5M H_2SO_4	278	40.8	4 h @ 10 mA cm^{-2}	9
Ru NCs/Co_2P	0.5M H_2SO_4	197	89	10 h @ 12 mA cm^{-2}	10
Ru@IrO_x	0.05M H_2SO_4	282	69.1	24 h @ 1.55 V vs. RHE	11

Mg-doping RuO_2	**0.5M H_2SO_4**	**228**	**48.66**	**30 h @ 10 mA cm-2**	**12**
Ni-Ru@ RuOx-HL	**0.5M H_2SO_4**	**184**	**44**	**30 h @ 10 mA cm-2**	**13**
IrO_2–BN-rGO	**0.5M H_2SO_4**	**300**	**72.1**	**12350 cycles @ 0.30-0.33 V**	**14**
CP@NCNT	**0.5M H_2SO_4**	**317**	**75**	**24 h @ 1.565 V v.s. RHE**	**15**
Ultrafine Defective RuO_2	**0.5M H_2SO_4**	**179**	**36.9**	**20 h @ 10 mA cm^{-2}**	**16**
$Mn_{0.73}Ru_{0.27}O_{2-\delta}$	**0.5M H_2SO_4**	**208**	**65.3**	**10 h@10 mA cm^{-2}**	**17**

References

1. W. Sun, Y. Song, X. Q. Gong, L. M. Cao and J. Yang, *Chem Sci*, 2015, **6**, 4993-4999.
2. T. Audichon, T. W. Napporn, C. Canaff, C. Morais, C. Comminges and K. B. Kokoh, *The Journal of Physical Chemistry C*, 2016, **120**, 2562-2573.
3. T. Bhowmik, M. K. Kundu and S. Barman, *ACS Appl Mater Interfaces*, 2016, **8**, 28678-28688.
4. L. Fu, P. Cai, G. Cheng and W. Luo, *Sustainable Energy & Fuels*, 2017, **1**, 1199-1203.
5. L. Fu, G. Cheng and W. Luo, *Journal of Materials Chemistry A*, 2017, **5**, 24836-24841.
6. J. Zhang, G. Wang, Z. Liao, P. Zhang, F. Wang, X. Zhuang, E. Zschech and X. Feng, *Nano Energy*, 2017, **40**, 27-33.
7. Z. Fan, J. Jiang, L. Ai, Z. Shao and S. Liu, *ACS Appl Mater Interfaces*, 2019, **11**, 47894-47903.
8. H.-S. Park, J. Yang, M. K. Cho, Y. Lee, S. Cho, S.-D. Yim, B.-S. Kim, J. H. Jang and H.-K. Song, *Nano Energy*, 2019, **55**, 49-58.
9. Q. Feng, J. Zou, Y. Wang, Z. Zhao, M. C. Williams, H. Li and H. Wang, *ACS Appl Mater Interfaces*, 2020, **12**, 4520-4530.
10. Y. Deng, L. Yang, Y. Wang, L. Zeng, J. Yu, B. Chen, X. Zhang and W. Zhou, *Chinese Chemical Letters*, 2021, **32**, 511-515.
11. J. Shan, C. Guo, Y. Zhu, S. Chen, L. Song, M. Jaroniec, Y. Zheng and S.-Z. Qiao, *Chem*, 2019, **5**, 445-459.

12. Y. Li, L. Xing, D. Yu, A. Libanori, K. Yang, J. Sun, A. Nashalian, Z. Zhu, Z. Ma, Y. Zhai and J. Chen, *ACS Applied Nano Materials*, 2020, **3**, 11916-11922.
13. A. M. Harzandi, S. Shadman, A. S. Nissimagoudar, D. Y. Kim, H. D. Lim, J. H. Lee, M. G. Kim, H. Y. Jeong, Y. Kim and K. S. Kim, *Advanced Energy Materials*, 2021, **11**.
14. P. Joshi, R. Yadav, M. Hara, T. Inoue, Y. Motoyama and M. Yoshimura, *Journal of Materials Chemistry A*, 2021, **9**, 9066-9080.
15. D. Yang, W. Hou, Y. Lu, W. Zhang and Y. Chen, *Journal of Energy Chemistry*, 2021, **52**, 130-138.
16. R. Ge, L. Li, J. Su, Y. Lin, Z. Tian and L. Chen, *Advanced Energy Materials*, 2019, **9**.
17. K. Wang, Y. Wang, B. Yang, Z. Li, X. Qin, Q. Zhang, L. Lei, M. Qiu, G. Wu and Y. Hou, *Energy & Environmental Science*, 2022, **15**, 2356-2365.